

Crystallization and preliminary X-ray diffraction studies of the FimC–FimH chaperone–adhesin complex from *Escherichia coli*

STEFAN KNIGHT,^a MATTHEW MULVEY^{a,b} AND JEROME PINKNER^b at ^a*Department of Molecular Biology, Swedish University of Agricultural Sciences, Uppsala Biometical Centre, PO Box 590, S-751 24 Uppsala, Sweden.* and ^b*Department of Molecular Microbiology, Washington University School of Medicine, St Louis, Missouri 63110-1093, USA.*
E-mail: stefan@xray.bmc.uu.se

(Received 4 June 1996; accepted 17 September 1996)

Abstract

A complex of the periplasmic chaperone FimC and the mannose-binding adhesin FimH from the *Escherichia coli* type 1 pilus system has been crystallized from ammonium sulfate solution using the hanging-drop vapour-diffusion method. The crystals diffract to a minimum Bragg spacing of 2.7 Å and belong to the space group $P4_12_12$, or $P4_32_12$ with cell dimensions $a = b = 97.7$, $c = 215.9$ Å at room temperature. Data to 3.0 Å have been collected from a single crystal frozen to $T = 100$ K.

1. Introduction

All living cells interact with other cells in one way or another. For example, within multicellular organisms, cells interact with similar types of cells to form the organ tissues of the body. Bacterial cells interact with each other (*e.g.* conjugation) and, in the case of commensal or pathogenic bacteria, with target host cells.

Pathogenic bacteria utilize a number of strategies to recognize and colonize target tissues. The common theme is that proteins on the bacterial surface called adhesins recognize surface elements, often carbohydrates, on the surface of the target cells. Binding to the target cells (adhesion) is the first, crucial step in colonization and may trigger a cascade of chemical signalling processes between the bacterium and the target cell (Blikska, Galán & Falkow, 1993). The specific stereochemical fit between the bacterial adhesin molecule and the receptor determines the host range, tissue and cell tropisms of the bacteria, and allows colonization of tissue where the bacteria would otherwise not adhere.

Bacterial adhesins are often assembled into hair-like fibers called fimbriae or pili (Hultgren *et al.*, 1993). Such fibers are usually comprised of structural proteins that have the apparent function of serving as a pedestal for adhesin presentation. Often the adhesins are components of specialized structures called tip fibrillae that are joined to the distal ends of thicker pilus rods. Some proteins serve as both the structural component of the pilus fiber and the adhesin. Adhesive pili range in diameter from 20 to 100 Å, whereas other adhesive organelles are very thin (< 20 Å) fibrillar structures. Such thin fibers tend to coil up into a fuzzy adhesive mass (referred to as a capsular antigen, thin aggregative pili, or curli) on the surface of the bacterium. In addition, there are also many examples of adhesins that are not part of any known oligomeric structures. These adhesins are typically referred to as non-pilus associated adhesins.

A general feature of many attachment organelle systems from Gram-negative bacteria is that they require a two-

component assembly system for their development (Jacob-Dubuisson, Kuehn & Hultgren, 1993). These highly conserved assembly systems consist of periplasmic immunoglobulin-like chaperones (Holmgren, Kuehn, Brändén & Hultgren, 1992; Hultgren *et al.*, 1993; Hung, Knight, Woods, Pinkner, 1996) and outer membrane associated ushers (Dodson, Jacob-Dubuisson, Striker & Hultgren, 1993). The usher molecules are large proteins that are involved in export of organelle subunits and may also function as platforms for organelle assembly. Periplasmic chaperones bind to interactive surfaces on nascent subunit proteins to promote their correct folding and to prevent their non-productive aggregation in the periplasm. Chaperone-subunit complexes are targeted to the usher where subunits are dissociated from the chaperone and incorporated into pili in a defined order. The structure of the chaperone from the *E. coli* P pilus system, PapD, has been determined by X-ray crystallography (Holmgren & Brändén, 1989), and is the prototype member of a growing family of periplasmic chaperones. The molecule is folded like two immunoglobulin domains oriented at an angle to each other forming a deep cleft between the domains. The highly conserved cleft was shown by mutagenesis studies to contain the subunit binding site (Slonim, Pinkner, Brändén & Hultgren, 1992). Subsequent crystallographic investigations of the chaperone cocrystallized with peptides corresponding to the COOH terminus of pilus subunits established parts of the molecular basis of chaperone-subunit interactions (Kuehn *et al.*, 1993; Hung *et al.*, 1996). However, no structure of a chaperone-subunit complex has so far been determined.

Type 1 pili which mediate binding to mannose-containing glycoproteins on eukaryotic cell surfaces are produced by nearly all *Enterobacteriaceae* (Brinton, 1965). The major component of type 1 pili is repeating FimA subunits arranged in a right-handed helix to form a 70 Å wide pilus rod with an axial hole. The adhesin, FimH (Klemm & Christiansen, 1987), is the major component of a thin (30 Å) tip fibrillum joined end-to-end to the distal end of the pilus rod (Jones *et al.*, 1995). Apart from FimA and the FimH adhesin, type 1 tip fibrillae also contain small amounts of the minor pilus components FimF and FimG. Type 1 pili are assembled via the chaperone/usher pathway with FimC being the chaperone (Jones *et al.*, 1993) and FimD the usher (Klemm & Christiansen, 1990). The amino-acid sequences of both FimC (Jones *et al.*, 1993) and FimH (Klemm & Christiansen, 1987) are known. The mature FimC chaperone comprises 205 amino acids ($M_r = 26$ kDa) and is 30% identical to PapD. FimC can thus be expected to have the same general fold as PapD. FimH, which has a length of 277 amino-acid residues ($M_r = 29$ kDa), may be divided into a C-terminal pilin-like

domain, and an N-terminal carbohydrate-binding domain (Jones *et al.*, 1995). Like all chaperone/usher-assembled pilins, FimH has a conserved beta-zipper motif (Hung *et al.*, 1997) at the COOH terminus required for proper interaction with the periplasmic chaperone. In this paper we present the crystallization and initial X-ray diffraction studies of a complex between the FimC chaperone and the FimH adhesin from the type 1 pilus system of *E. coli*.

The structure of the FimC-FimH chaperone-adhesin complex will provide a wealth of information relevant to both pilus assembly and pilus-mediated adhesion. The structure will reveal detailed information about the interaction between a periplasmic immunoglobulin-like chaperone and a target molecule. The surfaces that are capped by periplasmic chaperones upon binding to subunits are, at least in part, the same as those involved in subunit-subunit interactions in the adhesion organelle (Kuehn, Normark & Hultgren, 1991). The structure will thus also provide information about how subunits recognize and bind to each other in the pilus. The complex that we have crystallized was purified by mannose-Sepharose affinity chromatography with methyl- α -D-mannopyranoside as the eluant. This receptor analogue is, therefore, thought to be bound in the carbohydrate-binding site of the FimH adhesin. In addition to revealing the three-dimensional structure of a bacterial adhesin, the FimC-FimH structure may thus provide detailed information on the interaction between the adhesin and its receptor.

2. Experimental and results

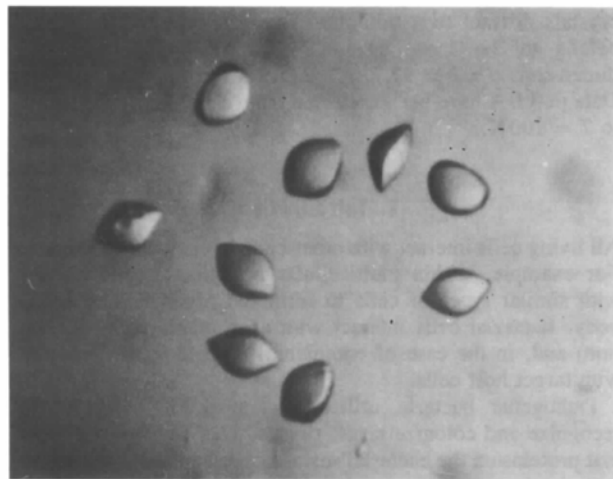
2.1. Protein purification and concentration

The FimC-FimH complex was expressed in *E. coli* and purified as previously described (Jones *et al.*, 1993). Purified FimC-FimH complexes were concentrated to about 5 mg ml^{-1} using Centricon 10 concentrators (Amicon Inc., USA). Initial attempts to concentrate the complex to above 1 mg ml^{-1} were unsuccessful and gave gelatinous precipitates. However, if the concentration procedure was interrupted and an early stage and the partially concentrated sample collected and centrifuged for 5 min at $3000g$ to remove precipitate, the concentration could be increased to more than 5 mg ml^{-1} without further precipitation. We have noted similar precipitation behavior upon concentration with several chaperone-subunit complexes that we are attempting to crystallize. Perhaps dissociation of the complex leads to non-specific aggregation of FimH which in turn forms a seed for further precipitation. If this initial precipitate is removed there will be excess free FimC chaperone in solution that could prevent further aggregation of transiently dissociating FimH by shifting the equilibrium in favour of complex formation. Dynamic laser light-scattering measurements on the concentrated protein sample show a monomodal distribution of particles with an estimated molecular weight of 58 kDa, close to that expected for a 1:1 complex of FimC-FimH (data now shown).

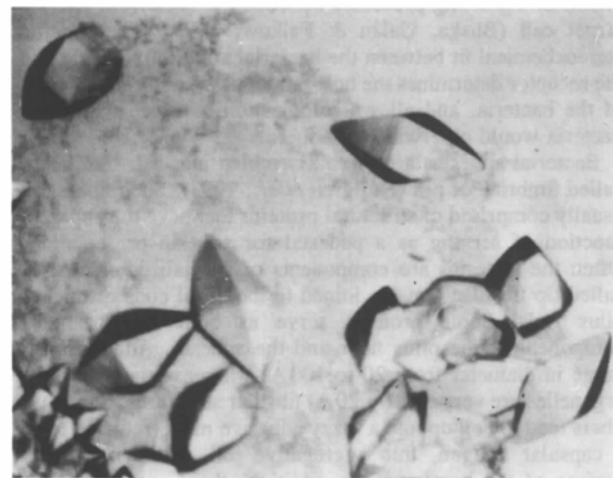
2.2. Crystallization

Crystals were grown using the hanging-drop method of vapour diffusion (McPherson, 1982) with ammonium sulfate as the precipitant. Rounded crystals showing obvious signs of disorder appeared after four months in drops containing $2 \mu\text{l}$ of protein at 1.2 mg ml^{-1} mixed with $2 \mu\text{l}$ of precipitant solution

consisting of 1.1 M (27% saturated) ammonium sulfate in 0.1 M Tris-HCl buffer at pH 8.3. Microseeding (Stura & Wilson, 1992) from these rounded crystals into drops that had been pre-equilibrated for several months produced well shaped but very small crystals (about $40 \mu\text{m}$ in the largest dimension). For production of diffraction-quality crystals, drops were set up by mixing $2 \mu\text{l}$ of protein at 5 mg ml^{-1} with $2 \mu\text{l}$ of reservoir solution containing ammonium sulfate at concentrations ranging from 0.4 to 0.9 M in 0.1 M Tris-HCl buffer (pH 7.9–8.5) and pre-equilibrated for 2 months and then streak seeded. Under these conditions the seeds are stable for several months but crystals do not grow. Crystal growth may then be induced by increasing the concentration of ammonium sulfate in the well to above 1.0 M . Crystals normally appear one to two days after boosting the ammonium sulfate concentration and continue to grow for one week and



(a)



(b)

Fig. 1. (a) Lentil-shaped crystals produced by microseeding from spontaneously grown disordered crystals. (b) Diamond-shaped crystals produced by the addition of various carbohydrates to the crystallization medium.

up to one month. For diffraction experiments small (<0.1 mm) well formed crystals (Fig. 1a) that had grown for about one week were selected. Crystals that continue to grow for longer than one week obtain a maximum size of about 0.2 mm in all directions but exhibit obvious growth defects and do not diffract to more than 10 Å resolution.

To test that the crystals did contain both FimC and FimH a few crystals were subjected to sodium dodecylsulfate–polyacrylamide gel electrophoresis (SDS–PAGE). Crystals were removed from the crystallization drop using a 1 mm glass capillary and then sequentially transferred to five 20 µl drops of 1.1 M ammonium sulfate in 0.1 M Tris–HCl buffer to remove any non-crystallized protein. The crystals were collected in a minimal amount of liquid and centrifuged at 1000g for 5 min. The supernatant was removed and the crystals dissolved in 10 µl double-distilled water prior to preparation for SDS–PAGE. The resulting gel (Fig. 2) clearly shows two bands corresponding to FimC and FimH (lane 2) whereas there is no protein in the final wash (lane 1).

2.3. X-ray analysis

Initial data collection and characterization of the crystals was carried out at the X11 beamline at DESY (Hamburg, Germany) using radiation of 0.927 Å wavelength. The diffraction limit of a fresh crystal was about 2.7 Å. However, given the rapid decrease in diffracted intensities in the 3.2–2.7 Å resolution shell, data collection was limited to 3.2 Å. Data were collected at 288 K from one crystal placed at $F = 410$ mm from a MAR imaging plate using 0.7° rotation per image, and processed with *DENZO* (Otwinowski, 1993). Autoindexing showed that the crystals belong to one of the space groups $P4_12_1$ or $P4_32_1$ with unit-cell dimensions $a = b = 97.7$, $c = 215.9$ Å. Since the crystals were not very stable in the beam we decided to attempt data collection under cryoconditions to limit radiation damage. These experiments were carried out at the tunable BL-19 beamline at ESRF (Grenoble, France). Using 30% glycerol as cryoprotectant, 3.0 Å data were collected from a single crystal frozen to 100 K using a MAR imaging-plate detector. As is often found, freezing resulted in a shrinking of the

unit cell with a reduction of the c axis to $c = 213.2$ Å. The final data set comprises 107 577 observations of 20 836 independent reflections corresponding to 97.1% of the possible data with $R_{\text{sym}} = 8.4\%$ and $\langle I/\sigma(I) \rangle = 9.2$.

Because of the small size and the relatively weak diffraction of the FimC–FimH crystals it has not been possible to screen for heavy-atom derivatives using a laboratory rotating-anode source. Therefore we attempted derivatization at the synchrotron in Grenoble. There are four cysteine residues in the complex and so, hoping to prepare a mercury derivative, a crystal was soaked in 2 mM ethyl mercuri thiosalicylate (EMTS) overnight. Setting the wavelength at $\lambda = 1.0$ Å, 76 886 measurements of 20 148 unique reflections (including 14 597 Bijvoet pairs) to 3.0 Å Bragg spacing were collected at $T = 100$ K with $R_{\text{sym}} = 6.7\%$ and $\langle I/\sigma(I) \rangle = 12.0$. However, this crystal turned out not to provide a useful derivative with an anomalous signal of only 3.7% and isomorphous difference $R_{\text{iso}} = 14.5\%$. Although both the normal probability plot (Howell & Smith, 1992) and χ^2 analysis (Otwinowski, 1993) indicate some degree of binding, there are no significant features other than the origin peak in either the difference Patterson or the anomalous Patterson function calculated with these data. The data collected from the EMTS-soaked crystal thus constitute a second native data set.

The molecular weight of FimC is 26 kDa (Jones *et al.*, 1993) and that of FimH 29 kDa. This gives a V_m (Matthews, 1977) of $4.7 \text{ \AA}^3 \text{ Da}^{-1}$ for one FimC–FimH heterodimer in the asymmetric unit, or $2.3 \text{ \AA}^3 \text{ Da}^{-1}$ for two heterodimers in the asymmetric unit. There are no significant peaks other than those resulting from the crystallographic symmetry in the self rotation function calculated using either of the two data sets collected at the ESRF. However, native Patterson maps calculated using either of these data sets both contain a strong peak (about 17% of the origin peak) at $u = 0.24$, $v = 0.00$, $w = 0.50$. The asymmetric unit thus most likely contains two copies of a FimC–FimH heterodimer, related by a twofold axis parallel to the crystallographic c axis and passing through $x = 0.38$, $y = 0.00$ or $x = 0.00$, $y = 0.38$, giving rise to a strong translational peak in the Patterson function.

Recently, we have obtained crystals of selenomethionylated FimC–FimH that are isomorphous to the native crystals. We have also been able to significantly improve the size and quality of our crystals by addition of various carbohydrates to the crystallization medium. It is interesting to note that all of the additives that result in improved crystal quality have structural features in common with the mannose receptor. The improved crystal quality may thus be due to binding of carbohydrate additives in the receptor-binding pocket resulting in a stabilization of structural features in or around the pocket. The resulting diamond-shaped crystals (Fig. 1b), although still small, diffract to about 3.5 Å Bragg spacing on a rotating-anode source as compared to only 7 Å for the initial crystals. Using the improved crystals we are currently screening for heavy-atom derivatives. The crystals of selenomethionylated FimC–FimH will be used for MAD data collection.

This work was supported by grants to SK from the Swedish Research Council NFR and MedImmune Inc., USA. We thank the beamline staff at the EMBL (*c/o* DESY, Hamburg, Germany) and the BL-19 beamline at the ESRF (Grenoble, France) for help with the data collection.

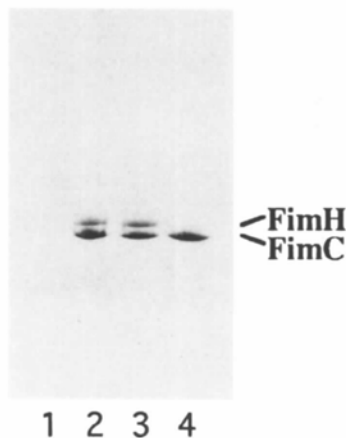


Fig. 2. SDS–PAGE gel of FimC–FimH crystals. Lane 1, final wash; lane 2, material from washed FimC–FimH crystals; lane 3, purified FimC–FimH control; lane 4, purified FimC control.

References

- Bliska, J. B., Galán, J. E. & Falkow, S. (1993). *Cell*, **73**, 903–920.
- Brinton, C. C. Jr (1965). *Trans. NY Acad. Sci.* **27**, 1003–1065.
- Dodson, K. W., Jacob-Dubuisson, F., Striker, R. T. & Hultgren, S. J. (1993). *Proc. Natl Acad. Sci. USA*, **90**, 3670–2674.
- Holmgren, A. & Brändén, C.-I. (1989). *Nature (London)*, **342**, 248–251.
- Holmgren, A., Kuehn, M. J., Brändén, C.-I. & Hultgren, S. J. (1992). *EMBO J.* **11**, 1617–1622.
- Howell, P. L. & Smith, G. D. (1992). *J. Appl. Cryst.* **25**, 81–86.
- Hultgren, S. J., Abraham, S., Caparon, M., Falk, P., St. Geme, J. W. III & Normark, S. (1993). *Cell*, **73**, 887–901.
- Hung, D., Knight, S. D., Woods, R., Pinkner, J. S. & Hultgren, S. J. (1996). *EMBO J.* **15**, 3792–3805.
- Jacob-Dubuisson, F., Kuehn, M. & Hultgren, S. (1993). *Trends Microbiol.* **1**, 50–55.
- Jones, C. H., Pinkner, J. S., Nicholes, A. V., Slonim, L. N., Abraham, S. N. & Hultgren, S. J. (1993). *Proc. Natl Acad. Sci. USA*, **90**, 8397–8401.
- Jones, C. H., Pinkner, J. S., Roth, R., Heuser, J., Nicholes, A. V., Abraham, S. N. & Hultgren, S. J. (1995). *Proc. Natl Acad. Sci. USA*, **92**, 2081–2085.
- Klemm, P. & Christiansen, G. (1987). *Mol. Gen. Genet.* **208**, 439–445.
- Klemm, P. & Christiansen, G. (1990). *Mol. Gen. Genet.* **220**, 334–338.
- Kuehn, M. J., Normark, S. & Hultgren, S. J. (1991). *Proc. Natl Acad. Sci. USA*, **88**, 10586–10590.
- Kuehn, M. J., Ogg, D. J., Kihlberg, J., Slonim, L. N., Flemmer, K., Bergfors, T. & Hultgren, S. J. (1993). *Science*, **262**, 1234–1241.
- McPherson, A. J. (1982). *Preparation and Analysis of Protein Crystals*, pp. 82–160. New York: John Wiley.
- Matthews, B. W. (1977). *The Proteins*, Vol. 3, edited by H. Neurath & R. L. Hill, pp. 403–590. New York: Academic Press.
- Otwinowski, Z. (1993). In *Data Collection and Processing. Proceedings of the CCP4 Study Weekend*, pp. 56–62. Warrington: Daresbury Laboratory.
- Slonim, L. N., Pinkner, J. S., Brändén, C.-I. & Hultgren, S. J. (1992). *EMBO J.* **11**, 4747–4756.
- Stura, E. A. & Wilson, I. A. (1992). In *Crystallization of Nucleic Acids and Proteins*, edited by A. Ducruix & R. Giegé. Oxford: IRL Press/Oxford University Press.